Desalination and Water Treatment
www.deswater.com

doi: 10.1080/19443994.2013.771286

51 (2013) 7145–7156
November

Removal of nitrate and phosphate anions from aqueous solutions using strong base anion exchange resin

A. Sowmya, S. Meenakshi*

Department of Chemistry, Gandhigram Rural Institute, Gandhigram, Tamilnadu, India
Email: drs_meena@rediffmail.com

Received 10 October 2012; Accepted 23 January 2013

ABSTRACT

The present study investigates the potential of a commercially available anion exchange resin namely Duolite A 171 (DA 171) as an adsorbent for the removal of nitrate and phosphate from the anionic aqueous solutions in batch mode. Effects of various parameters such as contact time, dosage of adsorbent, pH of the aqueous solutions, competitive co-anions, and temperature on the sorption capacity of the sorbent were studied. Adsorption from the nitrate/phosphate binary coexisting system was also done. Regeneration of the sorbent was carried out using 0.025 M NaCl solution. The desorption study showed that even after fifth regeneration cycle, the adsorption efficiency of DA 171 resin for nitrate and phosphate remained as 99.8 and 99.5%, respectively. The negative ΔH° values revealed that the adsorption of nitrate and phosphate is exothermic processes. Fitting of Langmuir, Freundlich, and Dubinin–Radushkevich (D–R) adsorption models to the equilibrium data were investigated. The adsorption capacity of nitrate (Q°) derived from Langmuir isotherm was 123.63 mg/g and of phosphate derived from D–R isotherm was 43.95 mg/g. The pseudo-second-order and particle diffusion kinetic models were the applicable kinetic models in both the cases. The adsorbent was characterized using scanning electron microscopy, energy-dispersive X-ray spectroscopy, and Fourier transform infrared spectroscopy.

Keywords: Phosphate; Nitrate; Duolite A 171; Regeneration; Isotherms

1. Introduction

Phosphate and nitrate are the key nutrients for the growth of biological organisms. The fertilizers having nitrate and phosphate in their composition really turned over the agricultural growth. Excess of these nutrients in water sources mainly induced by agricultural runoff, household wastes, and industrial effluents results in the decline of aquatic life and threatens the human health following the food chain. These nutrients especially phosphate in water sources induce eutrophication which leads to the overgrowth of phytoplankton, causing lack of oxygen, water quality reduction, and aquatic life depopulation [1]. The primary health hazards from drinking water with nitrate occurs when nitrate is transformed to nitrite in the digestive system which creates the condition known as methemoglobinemia which commonly observed among children [2]. A high concentration of nitrate in drinking water leads to the production of nitrosamine, which is related to cancer [3]. According to environmental protection agency (EPA), the maximum

---

*Corresponding author.

permissible level of phosphates in water is 0.1 mg/L [4] and that of nitrate is 45 mg/L [5].

Biological method [6], ion exchange [7], chemical reduction of nitrate [8,9], chemical precipitation of phosphate [10], electrocoagulation [11,12], membrane process [13,14], and adsorption method [15] are the common techniques used for the removal of nitrate and phosphate from water. Biological nutrient removal is a conventional method and nutrient can be removed from the effluents and aquaculture effectively. But additional organic substrates are required and temperature should be maintained [16–18]. Post-treatment is required due to micro-organisms [19]. Anion removal by adsorption through ion exchange mechanism is an effective, simpler, and economical method. The adsorbents can be efficiently reused by regenerating it using suitable eluents. Some of the resins used for the removal of nitrate and phosphate and their adsorption capacities are given in Table 1.

Duolite A 171 (DA 171) is a macro porous strong base anion exchange resin with quaternary ammonium functional group and Cl^- as the exchangeable anion. It has the matrix of styrene–divinylbenzene copolymer, and has not been studied for nitrate and phosphate removal so far. The present study evaluates the sorption behavior of nitrate and phosphate over DA 171 adsorbent using batch studies. In doing so, the effects of contact time, initial concentration of adsorbates, temperature of solution, adsorbent dosage, initial pH of solutions, and coexistent anions were investigated. The sorption studies from the binary aqueous solutions of nitrate and phosphate were also carried out. The best fit sorption isotherms among Freundlich, Langmuir, and D–R have been discussed. Thermodynamic parameters such as ΔG^o, ΔH^o, and ΔS^o were calculated in order to understand the nature of sorption process. Reaction-based and diffusion-based kinetic models were also discussed.

2. Materials and methods

2.1. Materials

The adsorbent DA 171 was supplied by Auchtel Products Ltd., Mumbai, India. It has been selected because of its low cost compared to other commercially available adsorbents. The characteristics of resin given by the formulaters along with pH at zero point charge (pH_{ZPC}) measured by drift method [27] are given in the Table 2. Working solution of nitrate and phosphate were prepared by dissolving respective KNO_3 and KH_2PO_4 (supplied by Merck) in deionized water. The reagents HCl, NaOH, NaCl, $NaHCO_3$, and Na_2SO_4 used were of analytical grade.

2.2. Instrumental characterization

Scanning electron microscopy (SEM) and energy-dispersive X-Ray spectroscopy (EDAX) were taken for the resin DA 171 on VEGA3TESCAN fitted with Bruker Nano GmbH, Germany. SEM image and EDAX spectra along with the percentage of elements present in the DA 171 resin at a particular focusing area are shown in Fig. 1(a) and (b). Fourier transform infrared (FTIR) spectra were collected on JASCO-460 plus model. DA 171 before and after treatment with nitrate and phosphate were ground with spectral grade KBr and made into pellets. All FTIR measurements were carried out at room temperature.

2.3. Adsorption and regeneration studies

The effect of contact time on nitrate and phosphate removal was investigated using 200 mg/L of nitrate solution and 50 mg/L phosphate solution, respectively, at room temperature in mechanical shaker having 120 rpm. The dose of the adsorbent used was 0.1 g in both the cases. pH of the nitrate and phosphate aqueous solutions as such was between 5 and 5.5. No pH adjustments were made. The concentrations of the nitrate solutions were varied between 100 and 500 mg/L, and that of phosphate solutions were 50–250 mg/L to study the effect of initial concentration. Contact time was fixed as 30 and 90 min for nitrate and phosphate, respectively. Dosage effect of DA 171 was investigated by varying the dose between 0.1 and 0.5 g. To investigate the pH effect, adsorption studies were carried out after adjusting the pH of the nitrate and phosphate solutions as 3,5,7,9, and 11 using concentrated HCl and NaOH. Adsorption isotherm and kinetic studies were carried out at 303, 313, and 323 K at various concentrations. Nitrate is analyzed by Ultraviolet Spectrophotometric Screening method in which the absorbance was measured at wavelength of 202 nm and phosphate is analyzed by Vanadomolybdophosphoric Acid Colorimetric method in which the absorbance was measured at wavelength of 400 nm [28] in a UV–Visible spectrophotometer (Spectroquant Pharo 300, Merck). The sorption studies from the nitrate/phosphate binary coexisting system were also carried out at various concentrations, and the nitrate and phosphate were analyzed using 883 Basic IC Plus Ion Chromatogram, Metrohm. pH of the solutions were analyzed using expandable ion analyzer, Orion EA940.

Regeneration of DA 171 after the adsorption studies of both nitrate and phosphate were carried out using 0.025 M NaCl at various contact times. The efficiency of the regenerated samples was checked up to fifth cycle.

Table 1
Resins used for the removal of nitrate and phosphate and their adsorption capacities

Resin	Polymeric matrix	Functional group and ionic form	Adsorbate	Adsorption capacity (mg/g)	Regenerant	Reference
Purolite A 520E	Polystyrene cross-linked with DVB	Quaternary ammonium and Cl^-	Nitrate	81.97	0.6 M NaCl	[20]
Amberlite IRA 400	Poly(styrene-divinylbenzene)	Quaternary ammonium and Cl^-	Nitrate	65.36	–	[21]
D-201	Poly(styrene-divinylbenzene)	Quaternary ammonium and Cl^-	Phosphate	12.2 mg P/g	–	[22]
HFO-201	Hydrated ferric oxide (HFO) impregnated poly(styrene-divinylbenzene)	Quaternary ammonium and HFO	Phosphate	17.8 mg P/g	5% NaOH + 5% NaCl	[22]
Amberlite IRN 9766	PS-DVB	Quaternary ammonium and Cl^-	Nitrate	192.8	–	[23]
Amberlite IRN 9766	PS-DVB	Quaternary ammonium and OH^-	Nitrate	190.6	–	[23]
Indion NSSR	Styrene divinyl benzene copolymer	Quaternary ammonium and Cl^-	Nitrate	119	–	[24]
ALR-AE resin	Hydrophyte *Arundo donax* L. reed	Amines	Nitrate	44.61	–	[25]
MIEX resin	Magnetized iron oxide incorporated into the polyacrylic matrix	Strong-base and Cl^-	Phosphate	26.5	–	[1]
NDP-2	Styrene–divinylbenzene	Quaternary ammonium and Cl^-	Nitrate	174.20	0.6 M NaCl	[26]
Purolite A 300	Gel polystyrene crosslinked with divinylbenzene	Quaternary ammonium and Cl^-	Nitrate	147.4	–	[26]
D 201	Styrene divinylbenzene	Quaternary ammonium and Cl^-	Nitrate	173.80	–	[26]
Duolite A 171	Styrene–divinylbenzene	Quaternary ammonium and Cl^-	Nitrate	123.63	0.025 M NaCl	Present study
Duolite A 171	Styrene–divinylbenzene	Quaternary ammonium and Cl^-	Phosphate	43.95	0.025 M NaCl	Present study

3. Results and discussion

3.1. FTIR studies

The FTIR of the DA 171, nitrate, and phosphate adsorbed DA 171 are given in Fig. 2. The characteristic peaks of styrene-divinylbenzene copolymer were observed. The peaks at 3,019 and 2,925 cm^{-1} are due to the stretching vibrations of C–H in ring and $-CH_2$ of the cross-linked polystyrene, respectively. The deformation vibrations of 1, 4-disubstituted benzene ring is due to the styrene-divinylbenzene matrix of resin which observed at 977 and 829 cm^{-1} [29]. The band at 1,481 cm^{-1} is due to symmetric deformation and asymmetric angular bending of methyl groups of quaternary nitrogen [30,31]. A sharp band at 1,382 cm^{-1} in the nitrate adsorbed DA 171 corresponds to the nitrate group [32,33]. The peak at

Table 2
Characteistics of the resin

Matrix	Styrene–divinylbenzene copolymer
Functional groups	$–N–(CH_3)_3$
Ionic form	Cl^-
Total capacity	Min 1.0 eq/L (Cl^- form)
Particle size	0.3–1.2 mm
pH_{ZPC}	7.1

1,074 cm^{-1} is due to the presence of phosphate anion in the phosphate adsorbed DA 171 [3].

3.2. Effect of contact time, adsorbate concentration and dose of the adsorbent

The sorption capacity and required contact time are important factors in the adsorption process since it decides the applicability of the adsorbent. Nitrate sorption on DA 171 was fast. Around 62 mg/g of sorption capacity was attained in 10 min and was saturated in approximately 30 min with a sorption capacity of 78 mg/g. While phosphate sorption was slow compared to nitrate sorption and the process extend over 30 min to reach the sorption capacity of 14.7 mg/g and 90 min to reach the saturation with a sorption capacity of 17.5 mg/g (Fig. 3). The batch studies were carried by with varying the initial concentrations of aqueous anionic solutions (Fig. 4(a) and (b). The sorption of nitrate and phosphate increased with increasing initial concentration of the solutions which shows the strong adsorption capability of the resin. With increasing concentration of the solutions, more ions came to the internal parts of the DA 171 through diffusion. In drinking water, the presence of nitrate and phosphate is normally less than 50 and 10 mg/L, respectively. About 50 mg/L of nitrate and 10 mg/L of phosphate synthetic solutions were used for sorption studies and almost 99% removal was observed in both the cases. There was an increase in the anion removal percentage with the increase of sorbent dose. But, after 0.2 mg, the increase in the dose does not significantly alter the anionic sorptions (Fig. 5).

3.3. Effect of pH

pH is an important parameter which alters the adsorbate as well as adsorbent nature [34]. From the results shown in Fig. 6, it is evident that the nitrate adsorption took place well at the pH ranges of 3–9. But at pH 11, the competition of OH^- with nitrate anions leads to decline in the sorption capacity [35]. In contrast, as the pH of the solution increase the phosphate sorption capacity also increased and reached a maximum of 25 mg/g at basic pH of 11. This is due to the existence of phosphate in various ionic forms at different pH levels. Phosphate can exist in the form of H_3PO_4, $H_2PO_4^-$, HPO_4^{2-}, and PO_4^{3-}, respectively, at pHranges of <2, 2–7, 7–12.5, and >12.5 [36]. Thus as the pH of the solution increase, the presence of divalent mono hydrogen phosphate anion become predominant species in the solution which has higher charge (HPO_4^{2-}) than the monovalent dihydrogen phosphate anion ($H_2PO_4^-$) [4] and get exchanged more.

3.4. Adsorption from the nitrate/phosphate binary coexisting system

The adsorption studies were carried out from the binary coexisting solution of nitrate and phosphate anions. Three solutions were prepared with the concentration of ions as 200 mg/L of nitrate; 200 mg/L phosphate and 50 mg/L of nitrate; 50 mg/L phosphate and 200 mg/L of nitrate; 50 mg/L phosphate. In the three cases, the sorption capacities were 78.6 mg/g; 17.5 mg/g and 21.2 mg/g; 12.2 mg/g and 69.1 mg/g; 10.5 mg/g, respectively (Fig. 7). As the concentration varies, the availability of the ions at the sorption sites is also varies. And also from the effect of contact time studies it was evident that nitrate adsorption on the resin is rapid and more effective than the phosphate adsorption. Though the resin is more selective towards nitrate, phosphate adsorption is also significant.

3.5. Effect of co-ions

Anions such as Cl^-, HCO_3^-, and SO_4^{2-} are mostly found in natural fresh water and effluent water. The adsorption abilities of the DA 171 for nitrate and phosphate removal in the presence and absence of Cl^-, HCO_3^-, and SO_4^{2-} ions are shown in Fig. 8. It can be seen that in the presence of 200 mg/L of Cl^-, HCO_3^-, and SO_4^{2-} anions, nitrate removal capacity was 58.1, 65.5, and 47.3 mg/g, respectively, and phosphate removal capacity was 12, 18.5, and 4.5 mg/g, respectively. Higher influence of sulfate on the adsorption was due to its higher ionic charge than nitrate and phosphate ions [15,37].

3.6. Isotherms

The equilibrium sorption data of nitrate and phosphate on adsorption models viz., Langmuir, Freund-

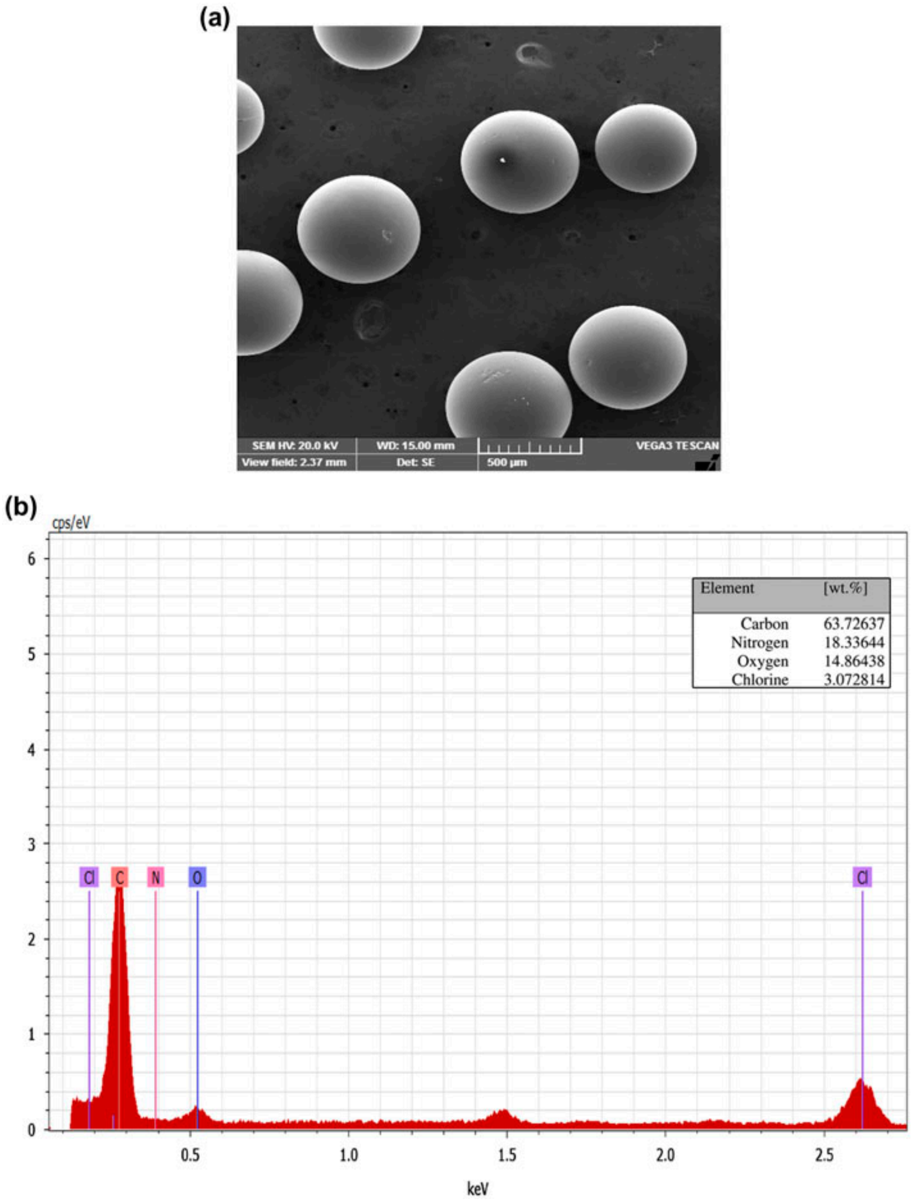

Element	[wt.%]
Carbon	63.72637
Nitrogen	18.33644
Oxygen	14.86438
Chlorine	3.072814

Fig. 1. (a) SEM images of DA 171 and (b) EDAX and elemental composition.

lich, and Dubinin–Radushkevich (D–R) adsorption models were investigated and the equations are as follows.

The linear form of Freundlich equation [38] is,

$$\log q_{\mathrm{e}} = \log k_{\mathrm{F}} + \frac{1}{n}\log C_{\mathrm{e}}$$

where C_{e} is the equilibrium concentration (mg/L) and q_{e} is the amount adsorbed per unit weight of adsorbent. The k_{F} and n values are calculated from the intercepts and slopes of the linear plots of log q_{e} vs. log C_{e} for the removal of both anions.

The linear form of Langmuir equation [39] is given as follows:

$$(C_{\mathrm{e}}/q_{\mathrm{e}}) = (1/Q_0 b) + (C_{\mathrm{e}}/Q_0)$$

where C_{e} is the equilibrium concentration (mg/L) and q_{e} is the amount adsorbed at equilibrium (mg/g) and Q_0 and b are Langmuir constants related to energy of adsorption (L/mg) and adsorption capacity (mg/g), respectively.

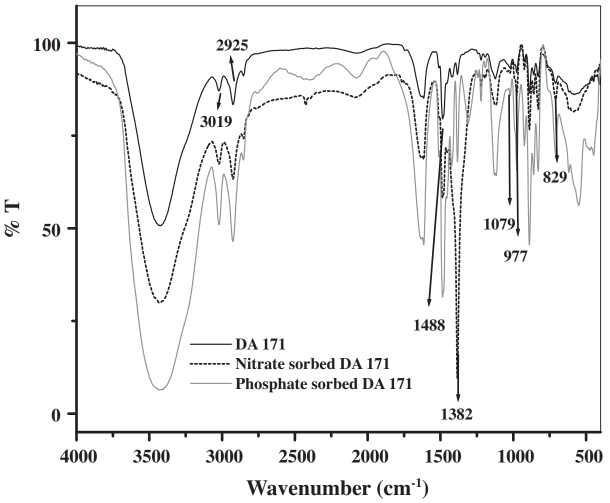

Fig. 2. FTIR spectra of DA 171 before and after the adsorption of nitrate and phosphate.

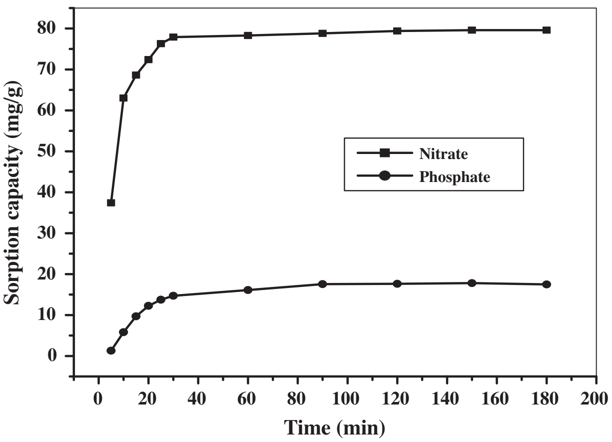

Fig. 3. Effect of contact time on removal of nitrate and phosphate.

The essential characteristics of the Langmuir isotherm can be expressed in terms of a dimensionless constant separation factor or equilibrium parameter, R_L [40].

$$R_L = \frac{1}{1 + bC_0}$$

where b is the Langmuir isotherm constant and C_0 is the initial concentration of anion (mg/L).

Linear form of D–R isotherm equation is given as,

$$\ln q_e = \ln X_m - k_{DR}\varepsilon^2$$

where X_m is the adsorption capacity (mg/g) and k is the constant related to adsorption energy (mol^2/kJ^2). The values of k and X_m were computed from the slope and intercept of the plot ln q_e vs. ε^2. Polanyi potential can be calculated by the equation,

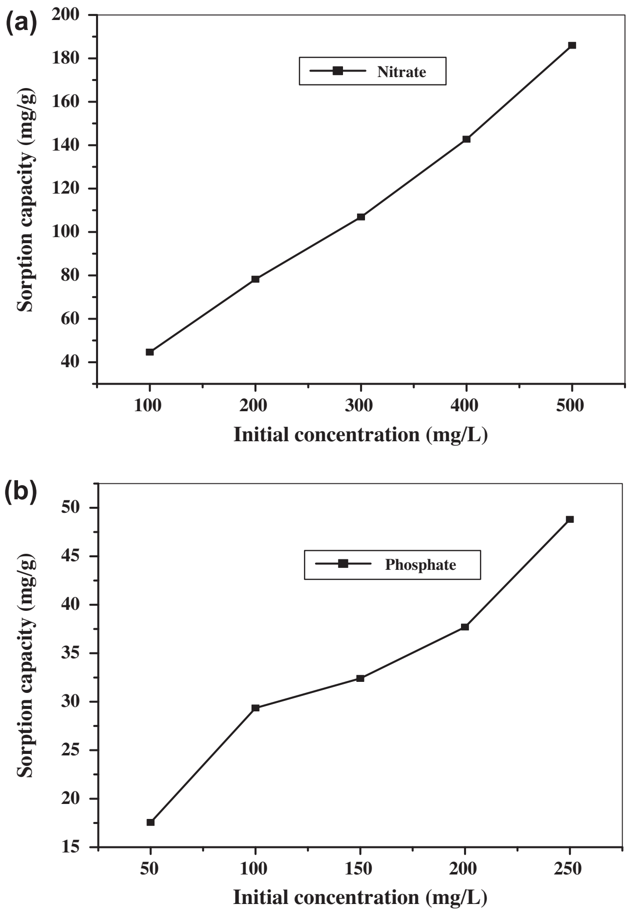

Fig. 4. (a) Effect of initial concentration on removal of nitrate and (b) effect of initial concentration on removal of phosphate.

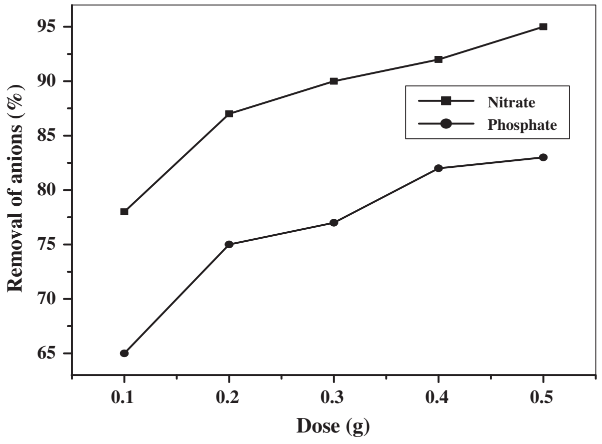

Fig. 5. Effect of dose of DA 171 on removal of nitrate and phosphate.

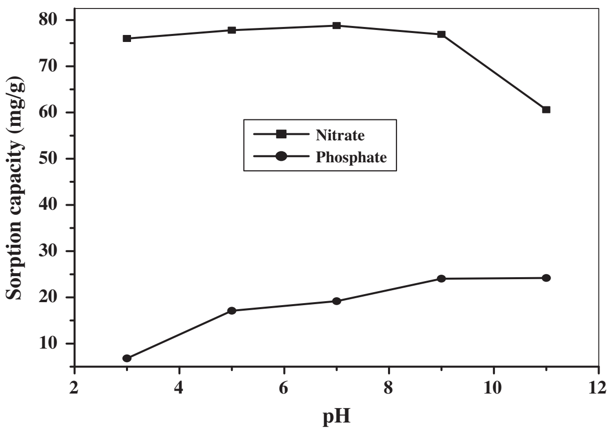

Fig. 6. Effect of pH on removal of nitrate and phosphate.

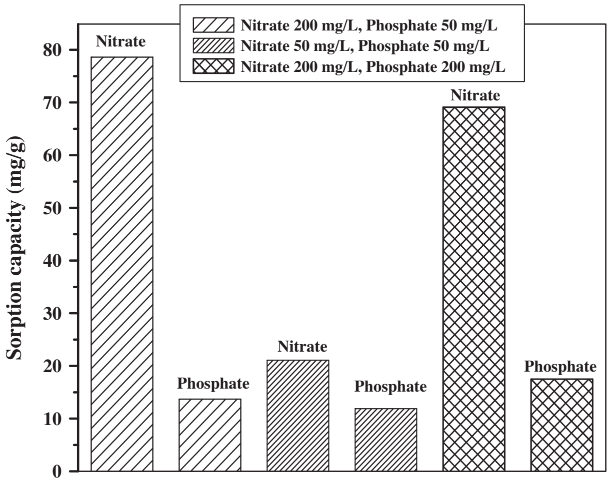

Fig. 7. Sorption from the nitrate/phosphate binary coexisting system.

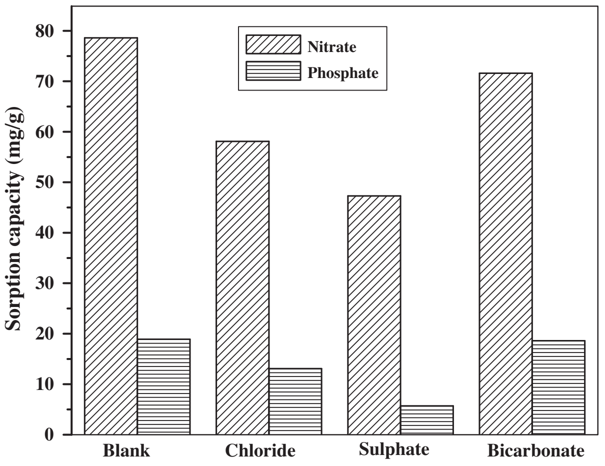

Fig. 8. Effect of co-ions on removal of nitrate and phosphate.

$$\varepsilon = RT\ln\left(1+\frac{1}{C_{\mathrm{e}}}\right)$$

where T is the temperature (K) and R is the gas constant (8.314 J mol^{-1} K^{-1}). The value of k is used to calculate the mean free energy E (kJ/mol) of the sorption,

$$E = -(2k)^{-0.5}$$

The parameters of adsorption isotherms studied for the data of nitrate and phosphate equilibrium studies carried out at 303 K are given in the Table 3. The values of $1 < n < 10$ [41] and R_{L} values between 0 and 1 indicate favorable adsorption [42] of both nitrate and phosphate. The higher r and lower sd values indicate the applicability of the three isotherms studied. To identify the most suitable isotherms for the adsorption of nitrate and phosphate onto DA 171, chi-square analysis was carried out. The mathematical statement of chi-square analysis [43] is

$$\chi^2 = \sum \frac{(q_{\mathrm{e}} - q_{\mathrm{e,m}})^2}{q_{\mathrm{e,m}}}$$

Table 3
Parameters for Freundlich, Langmuir, and D–R isotherms for the adsorption of nitrate and phosphate on DA 171

Adsorption isotherm	Parameters	Nitrate	Phosphate
Freundlich	$1/n$	0.406	0.632
	n	2.459	1.581
	k_{F} (mg/g) (L/mg)$^{1/n}$	15.048	0.164
	r	0.995	0.999
	sd	0.011	0.002
	χ^2	0.044	0.0002
Langmuir	Q_0 (mg/g)	123.06	33.400
	b (L/g)	0.031	0.011
	r	0.999	0.994
	sd	0.004	0.012
	R_{L}	0.110	0.627
	χ^2	0.015	32.813
Dubnin–Radushkevich	k_{DR} (mol^2/J^2)	2.02E−04	5.59E−05
	X_{m} (mg/g)	116.98	43.95
	E (kJ/mol)	0.050	0.095
	r	0.983	0.999
	sd	0.145	0.008
	χ^2	202.816	0.001

where $q_{e,m}$ is equilibrium capacity obtained by calculating from the model (mg/g) and q_e is experimental data of the equilibrium capacity (mg/g). The chi-square values obtained using the nonlinear forms of isotherms are given in the Table 3.

Freundlich > Langmuir >> D–R was the order of suitability in the case of nitrate sorption and for phosphate it was Freundlich > D–R >> Langmuir. Hence, the most suitable adsorption isotherm was Freundlich for both nitrate and phosphate adsorption and it can be concluded that, nonideal adsorption on the heterogeneous surface of DA 171 was occurred, and multilayer nitrate and phosphate sorption was also possible [24]. The E values obtained for nitrate and phosphate from the D–R isotherm were 0.050 and 0.095 kJ/mol, respectively, which further confirms the physical adsorption between the anions and functional moieties in DA 171 [44,45].

3.7. Thermodynamic parameters

The temperature dependence of adsorption process is associated with the changes in thermodynamic parameter such as standard free energy, enthalpy, and entropy of adsorption. These thermodynamic parameters were calculated by the Khan and Singh method [46] and given in the Table 4. The negative values of ΔG° at different temperatures indicate the spontaneous nature of phosphate and nitrate adsorption. The negative values of ΔH° confirm the exothermic nature of adsorption in both cases. The positive values of ΔS° indicated a decreased randomness during the adsorption of nitrate and phosphate onto DA 171.

3.8. Kinetic parameters

The reaction-based and diffusion-based models that are the two most important types of adsorption kinetic models were adopted to fit the experimental data of nitrate and phosphate adsorption on DA 171.

3.8.1. Reaction based models

The adsorption kinetic data were described by the Lagergren pseudo-first-order model [47], which is the earliest known equation describing the adsorption rate based on the adsorption capacity.

$$\log(q_e - q_t) = \log q_e - \frac{k_{ad}}{2.303} t$$

where q_e and q_t are the adsorption capacity at equilibrium and at time t, respectively (mg g^{-1}), k_{ad} is the rate constant of pseudo-first-order adsorption (min^{-1}). Linear plots of log $(q_e - q_t)$ against t give a straight line that indicates the applicability of pseudo-first-order model. k_{ad} and q_e can be determined from the slope and intercept.

The adsorption kinetics may be described by the pseudo-second-order model [48], which is generally given as follows

$$\frac{t}{q_t} = \frac{1}{h} + \frac{t}{q_e}$$

where $q_t = \frac{q_e^2 kt}{1+q_e kt}$, amount of anions on the surface of the sorbents at any time, t (mg/g), k is the pseudo-second-order rate constant (g/mg min), q_e is the amount anions adsorbed at equilibrium (mg/g) and the initial sorption rate, $h = kq_e^2$. The value of q_e (1/slope), k (slope^2/intercept), and h (1/intercept) of the pseudo-second-order equation can be found out experimentally by plotting t/q_t against t.

3.8.2. Diffusion-based models

The solute transfer is generally characterized either by particle diffusion or by intraparticle diffusion controls [49]. A simple equation for the particle diffusion controlled sorption process is as follows,

$$\ln(1 - \frac{C_t}{C_e}) = -k_p t$$

where k_p is the particle diffusion coefficient (mg/g min). The value of the particle diffusion coefficient is obtained by the slope of $\ln(1 - C_t/C_e)$ against t.

Table 4
Thermodynamic parameters for the adsorption of nitrate and phosphate on DA 171

Anion	ΔG° (kJ mol^{-1})			ΔH° (kJ mol^{-1})	ΔS° (kJ K^{-1} mol^{-1})
	303 K	313 K	323 K		
Nitrate	−11.18	−14.07	−14.98	−46.71	0.19
Phosphate	−8.98	−10.87	−7.92	−24.20	0.05

Table 5
Peudo-second-order kinetic and particle diffusion kinetic parameters of nitrate

Kinetic models	Parameters	303 K			313 K			323 K		
		150 mg/L	200 mg/L	250 mg/L	150 mg/L	200 mg/L	250 mg/L	150 mg/L	200 mg/L	250 mg/L
Pseudo-second-order	q_e (mg/g)	67.249	94.518	97.276	61.576	86.132	94.786	89.928	86.355	89.928
	k (g/mg min)	0.005	0.001	0.0032	0.002	0.0012	0.001	0.001	0.001	0.001
	h (mg/g min)	20.925	13.369	30.864	10.384	9.289	16.097	14.803	7.700	14.803
	R^2	0.997	0.992	0.997	0.998	0.978	0.994	0.993	0.990	0.993
	sd	0.011	0.014	0.007	0.012	0.025	0.012	0.014	0.017	0.014
Particle diffusion	k_p (min^{-1})	0.294	0.136	0.156	0.173	0.125	0.157	0.190	0.125	0.148
	R^2	0.956	0.987	0.987	0.992	0.967	0.987	0.989	0.994	0.989
	sd	0.826	0.217	0.267	0.207	0.336	0.321	0.260	0.134	0.314

Table 6
Peudo-second-order kinetic and particle diffusion kinetic parameters of phosphate

Kinetic models	Parameters	303 K			313 K			323 K		
		50 mg/L	60 mg/L	70 mg/L	50 mg/L	60 mg/L	70 mg/L	50 mg/L	60 mg/L	70 mg/L
Pseudo-second-order	q_e (mg/g)	18.021	21.978	25.793	17.702	20.308	23.501	15.590	17.914	21.491
	k (g/mg min)	0.004	0.004	0.003	0.003	0.003	0.003	0.001	0.002	0.001
	h (mg/g min)	1.358	2.075	2.507	0.985	1.424	2.121	0.362	0.648	0.910
	R	0.999	0.999	0.999	0.999	0.999	0.999	0.994	0.999	0.999
	sd	0.020	0.026	0.029	0.058	0.066	0.044	0.227	0.081	0.078
Particle diffusion	k_p (min^{-1})	0.040	0.051	0.043	0.053	0.037	0.037	0.048	0.039	0.039
	R	0.999	0.998	0.996	0.993	0.991	0.992	0.986	0.997	0.993
	sd	0.028	0.123	0.128	0.198	0.158	0.148	0.258	0.078	0.138

The intraparticle diffusion model used here refers to the theory proposed by Weber and Morris [49]. The intraparticle diffusion equation,

$$q_t = k_i t^{1/2}$$

where k_i is the intraparticle diffusion coefficient (mg/g min$^{0.5}$). The slope of the plot of q_t against $t^{1/2}$ will give the value of the intraparticle diffusion coefficient.

Among the two reaction-based models namely pseudo-first-order and pseudo-second-order models, the phosphate and nitrate adsorption kinetic data well fitted with the pseudo-second-order model with higher correlation co-efficient (r) [50]. And also particle diffusion was the applicable diffusion based kinetic model in both the cases. The values obtained are given in Tables 5 and 6 for nitrate and phosphate, respectively.

3.9. Regeneration studies

For regeneration, the important aspect is to return the polymeric material to its original state without altering its indented properties in order to make the process cost effective. The nitrate and phosphate adsorbed DA 171 resins were treated with 0.025 M NaCl solution for the time of 5, 10, 15, 30, and 60 min (Fig. 8(a)). Then the resins were washed with deionized water and dried in room temperature, and were used for the adsorption of nitrate and phosphate under predetermined conditions. It is evident that the DA171 was regenerated with Cl^- ions using the aqueous solution of 0.025 M of NaCl within 5 min. The sorption capacity of the resin towards the nitrate and phosphate adsorption was not altered. The regeneration studies were carried out up to fifth cycle (Fig. 8 (b)). The nitrate and phosphate sorption capacities remained 77.9 and 17.7 mg/g after fifth regeneration of the resin. DA 171 is an efficient reusable resin towards nitrate and phosphate. The sorption and desorption anions on the DA 171 can be depicted as follows (Fig. 9).

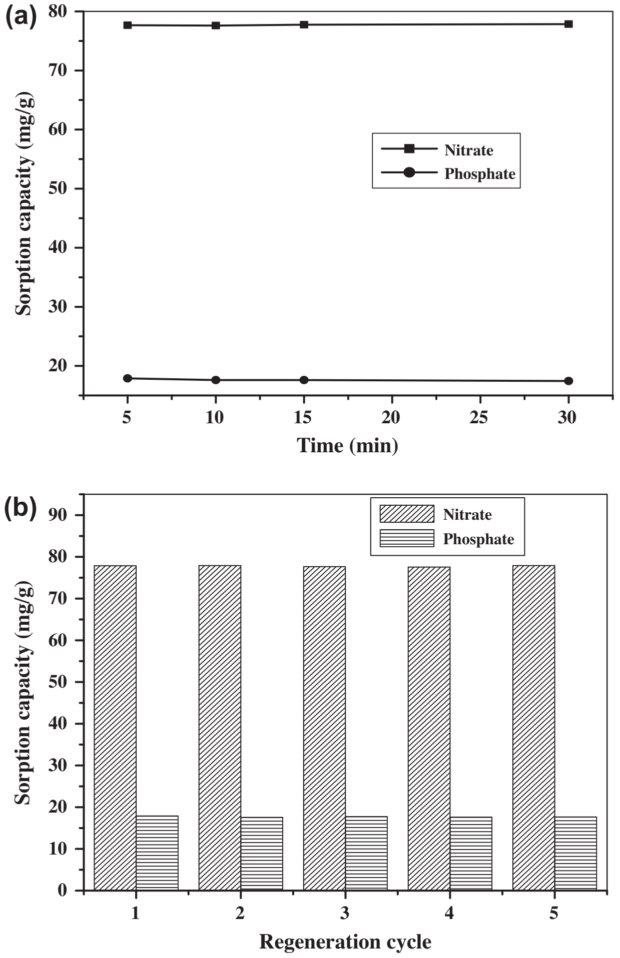

Fig. 9. (a) Effect of desorption time on the regeneration of nitrate and phosphate adsorbed DA 171 and (b) sorption capacity of regenerated DA 171 on nitrate and phosphate adsorption at various cycles.

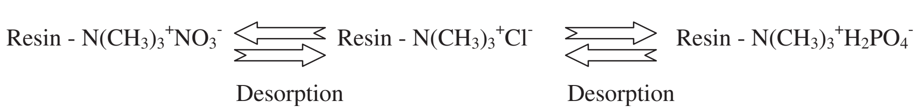

4. Conclusions

Uptake of nitrate is rapid and efficient than the uptake of phosphate on DA 171. Nitrate sorption was effective in the pH ranges of 3–9 and phosphate sorption was effective in the pH ranges 3–11 with an increase in SC at pH 11. In adsorption of both phosphate and nitrate, sulfate significantly altered the SC of the adsorbent. The adsorption isotherms were best fitted with the Freundlich adsorption isotherm which indicates the heterogeneous nature of sorption. Physical binding forces were involved in the sorption of both the anions on the resin which confirmed from E values calculated from D–R isotherm. The sorption of both nitrate and phosphate is exothermic and spontaneous. The kinetic data were well fitted with pseudo-second-order and particle diffusion models. The adsorption mechanism was due to ion exchange between chloride and the respective anions. The desorption rate is rapid and occurred within 5 min by using 0.025 M NaCl which would make the process cost effective, and hence the resin could be further employed for the technology development.

Acknowledgment

First author is thankful to UGC-BSR-RFSMS for the fellowship.

References

[1] L. Ding, C. Wu, H. Deng, X. Zhang, Adsorptive characteristics of phosphate from aqueous solutions by MIEX resin, J. Colloid Interf. Sci. 376 (2012) 224–232.

[2] A. Bhatnagar, E. Kumar, M. Sillanpääc, Nitrate removal from water by nano-alumina: Characterization and sorption studies, Chem. Eng. J. 163 (2010) 317–323.

[3] M.F.A. Taleb, G.A. Mahmoud, S.M. Elsigeny, E.-S.A. Hegazy, Adsorption and desorption of phosphate and nitrate using quaternary (polypropylene-g-N,N-dimethylamino ethylmethacrylate) graft copolymer, J. Hazard. Mater. 159 (2008) 372–379.

[4] K.S. Triantafyllidis, E.N. Peleka, V.G. Komvokis, P.P. Mavros, Iron-modified hydrotalcite-like materials as highly efficient phosphate sorbents, J. Colloid Interf. Sci. 342 (2010) 427–436.

[5] M.H. Ward, T.M. deKok, P. Levallois, J. Brender, G. Gulis, B. T. Nolan, J.V. Derslice, Workgroup report: Drinking-water nitrate and health—recent findings and research needs, Environ Health Perspect. 113 (2005) 1607–1614.

[6] J.P. Bassin, R. Kleerebezem, M. Dezotti, M.C.M. van Loosdrecht, Simultaneous nitrogen and phosphate removal in aerobic granular sludge reactors operated at different temperatures, Water Res. 46 (2012) 3805–3816.

[7] X. Xu, B.-Y. Gao, Q.-Y. Yue, Q.-Q. Zhong, Preparation of agricultural by- product based anion exchanger and its utilization for nitrate and phosphate removal, Biores. Technol. 101 (2010) 8558–8564.

[8] Y.H. Liou, S.L. Lo, C.J. Lin, C.Y. Hu, W.H. Kuan, S.C. Weng, Methods for accelerating nitrate reduction using zerovalent iron at near-neutral pH: Effects of H_2-reducing pretreatment and copper deposition, Environ. Sci. Technol. 39 (2005) 9643–9648.

[9] Y.M. Chen, C.W. Li, S.S. Chen, Fluidized zero valent iron bed reactor for nitrate removal, Chemosphere 59 (2005) 753–759.

[10] Y.H. Moon, J.G. Kim, J.S. Ahn, G.H. Lee, H.S. Moon, Phosphate removal using sludge from fuller's earth production, J. Hazard. Mater. 143 (2007) 41–48.

[11] E. Lacasa, P. Cãnizares, C. Sáez, F. J. Fernández , M. A. Rodrigo, Removal of nitrates from groundwater by electrocoagulation, Chem. Eng. J. 171 (2011) 1012–1017.

[12] S. Irdemez, Y.S. Yildiz, V. Tosunoğlu, Optimization of phosphate removal from wastewater by electrocoagulation with aluminum plate electrodes, Sep. Purific. Techn. 52 (2000) 6394–6401.

[13] J-H Ahn., K. Hochoo, H-S. Park, Reverse osmosis membrane treatment of acidic etchant wastewater: Effect of neutralization and polyelectrolyte coating on nitrate removal, J. Membrane Sci. 310 (2008) 296–302.

[14] E.N. Peleka, P.P. Mavros, D. Zamboulis, K.A. Matis, Removal of phosphates from water by a hybrid flotation-membrane filtration cell, Desalination 198 (2006) 198–207.

[15] R. Saad, K. Belkacemi, S. Hamoudi, Adsorption of phosphate and nitrate anions on ammonium-functionalized MCM-48: Effects of experimental conditions, J. Colloid Interf. Sci. 311 (2007) 375–381.

[16] H. Pahlavanzadeh, R. Katal, H. Mohammadi, Synthesize of polypyrrole nanocomposite and its application for nitrate removal from aqueous solution, J. Ind. Eng. Chem. 18 (2012) 948–956.

[17] S. Ghafari, M. Hasan, M.K. Aroua, Bio-electrochemical removal of nitrate from water and wastewater—A review, Bioresour. Technol. 99 (2008) 3965–3974.

[18] E. Arvin, D. Jenkins, Biological removal of phosphorus from wastewater, Crit. Rev. Env. Contr. 15 (1985) 25–64.

[19] A. Bhatnagar, M. Sillanpaa, A review of emerging adsorbents for nitrate removal from water, Chem. Eng. J. 168 (2011) 493–504.

[20] S. Samatya, N. Kabay, U. Yüksel, M. Arda, M. Yüksel, Removal of nitrate from aqueous solution by nitrate selective ion exchange resins, React. Funct. Polym. 66 (2006) 1206–1214.

[21] M. Chabani, A. Amrane, A. Bensmaili, Kinetics of nitrates adsorption on Amberlite IRA 400 resin, Desalination 206 (2007) 560–567.

[22] B. Pan, J. Wu, B. Pan, L. Lv, W. Zhang, L. Xiao, X. Wang, X. Tao, S. Zheng, Development of polymer-based nano sized hydrated ferric oxides (HFOs) for enhanced phosphate removal from waste effluents, Water Res. 43 (2009) 4421–4429.

[23] J. Dron, A. Dodi, Comparison of adsorption equilibrium models for the study of Cl^-, NO_3^- and SO_4^{2-} removal from aqueous solutions by an anion exchange resin, J. Hazard. Mater. 190 (2011) 300–307.

[24] S.N. Milmile, J.V. Pande, S. Karmakar, A. Bansiwal, T. Chakrabarti, R.B. Biniwale, Equilibrium isotherm and kinetic modeling of the adsorption of nitrates by anion exchange Indion NSSR resin, Desalination 276 (2011) 38–44.

[25] X. Xu, B. Gao, Y. Zhao, S. Chen, X. Tan, Q. Yue, J. Lin, Y. Wang, Nitrate removal from aqueous solution by *Arundo donax* L. reed based anion exchange resin, J. Hazard. Mater. 203–204 (2012) 86–92.

[26] H. Song, Y. Zhou, A. Li, S. Mueller, Selective removal of nitrate from water by a macroporous strong basic anion exchange resin, Desalination 296 (2012) 53–60.

[27] M.V.L. Ramon, F. Stoeckli, C.M. Castilla, F.C. Marin, On the characterization of acidic and basic surface sites on carbons by various techniques, Carbon 37 (1999) 1215–2121.

[28] APHA, Standard Methods for the Examination of Water and Waste Water, 21st ed., APHA, Washington, DC, 2005.

[29] B. Lee, L.-L. Bao, H.-J. Im, S. Dai, E.W. Hagaman, J.S. Lin, Synthesis and characterization of organic−inorganic hybrid mesoporous anion-exchange resins for perrhenate (ReO_4^-) anion adsorption, Langmuir 19 (2003) 4246–4252.

[30] A. Wołowicz, Z. Hubicki, Sorption of palladium(II) complexes onto the styrene–divinylbenzene anion exchange resins, Chem. Eng. J. 152 (2009) 72–79.

[31] M.R. Gandhi, G. Kalaivani, S. Meenakshi, Sorption of chromate and fluoride onto duolite a 171 anion exchange resin- a comparative study, Elixir Poll. 32 (2011) 2034–2040.

[32] M. Islam, R. Patel, Nitrate sorption by thermally activated Mg/Al chloride hydrotalcite-like compound, J. Hazard. Mater. 169 (2009) 524–531.

[33] J.T. Kloprogge, L. Hickey, R.L. Frost, The effect of varying synthesis conditions on zinc chromium hydrotalcite: A spectroscopic study, Mater. Chem. Phys. 89 (2005) 99–109.

[34] S. Meenakshi, N. Viswanathan, Identification of selective ion-exchange resin for fluoride sorption, J. Colloid Interf. Sci. 308 (2007) 438–450.

[35] M. Islam, R. Patel, Physicochemical characterization and adsorption behavior of Ca/Alchloride hydrotalcite-like compound towards removal of nitrate, J. Hazard. Mater. 190 (2011) 659–668.
[36] H. He, H. Kang, S. Ma, Y. Bai, X. Yang, High adsorption selectivity of ZnAl layered double hydroxides and the calcined materials toward phosphate, J. Colloid Interf. Sci. 343 (2010) 225–231.
[37] J. Zhang, Z. Shen, Z. Mei, S. Li, W. Wang, Removal of phosphate by Fe-coordinated amino-functionalized 3D mesoporous silicates hybrid materials, J. Environ. Sci. 23 (2011) 199–205.
[38] H.M.F. Freundlich, Uber die Adsorption im Losungen, Zeit. Phys. Chem. 57A (1906) 385–470.
[39] I. Langmuir, The constitution and fundamental properties of solids and liquids, J. Am. Chem. Soc. 38 (1916) 2221–2295.
[40] N. Viswanathan, S. Meenakshi, Synthesis of Zr(IV) entrapped chitosan polymeric matrix for selective fluoride sorption, Colloids Surf. B: Biointer. 72 (2009) 88–93.
[41] P. Ravichandran, A. Sowmya, S. Meenakshi, Equilibrium and kinetic studies on the removal of basic violet 10 from aqueous solutions using activated carbons prepared from industrial wastes, Bioremediation J. 16 (2012) 86–96.
[42] C.S. Sundaram, N. Viswanathan, S. Meenakshi, Uptake of fluorid by nano-hydroxyapatite/chitosan, a bioinorganic composite, Biores. Technol. 99 (2008) 8226–8230.
[43] Y.S. Ho, Selection of optimum sorption isotherm, Carbon 42 (2004) 2115–2116.
[44] A. Ozcan, A.S. Ozcan, S. Tunali, T. Akar, I. Kiran, Determination of the equilibrium, kinetic and thermodynamic parameters of adsorption of copper (II) ions onto seeds of Capsicum annuum, J. Hazard. Mater. B 124 (2005) 200–208.
[45] M.S. Onyango, Y. Kojima, O. Aoyi, E.C. Bernardo, H. Matsuda, Adsorption equilibrium modeling and solution chemistry dependence of fluoride removal from water by trivalent-cation exchange zeolite F-9, J. Colloid Interface Sci. 279 (2004) 341–350.
[46] A.A. Khan, R.P. Singh, Adsorption thermodynamics of carbofuran on Sn(IV) arsenosilicate in H^+, Na^+ and Ca^{2+} forms, Colloids Surf. 24 (1987) 33–42.
[47] S. Lagergren, Zur theorie der sogenannten adsorption gelöster stoffe, Kungliga Svenska Vetenskapsakademiens. Handlinger 24 (1898) 1–39.
[48] Y.S. Ho, C.C. Wang, Pseudo-isotherms for the sorption of cadmium ion onto tree fern, Process Biochem. 39 (2004) 761–765.
[49] W.J. Weber, J.C. Morris, Equilibria and capacities for adsorption on carbon, J. Sanitary. Eng. Div. 90 (1964) 79–107.
[50] G.N. Kousalya, M.R. Gandhi, S. Meenakshi, Preparation of modified chitin for the removal of chromium(VI), Bioremediation J. 14 (2010) 203–213.